JOC The Journal of Organic Chemistry

Article

pubs.acs.org/joc

Donor–Acceptor Ferrocenyl-Substituted Benzothiadiazoles: Synthesis, Structure, and Properties

Rajneesh Misra,* Prabhat Gautam, Thaksen Jadhav, and Shaikh M. Mobin

Department of Chemistry, Indian Institute of Technology Indore, Indore 452 017, India

Supporting Information

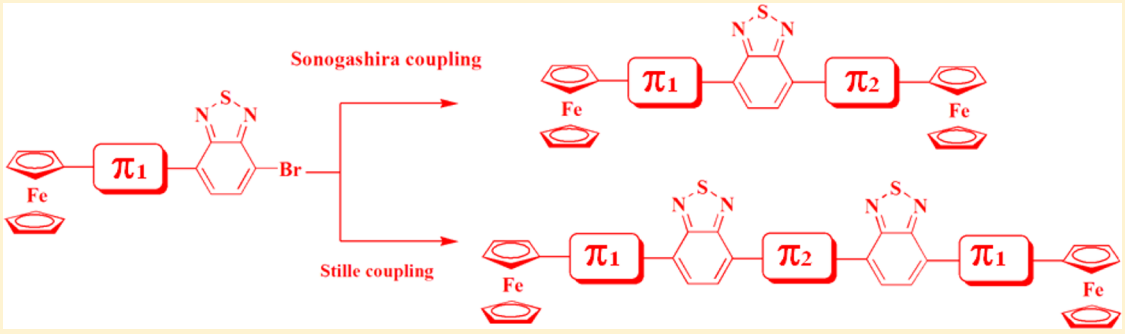

ABSTRACT: This article reports the design, and synthesis of D–π_1–A–π_2–D unsymmetrical, and D–π_1–A–π_2–A–π_1–D symmetrical type of ferrocenyl-substituted benzothiadiazoles by the Pd-catalyzed Sonogashira, and Stille coupling reactions. The photophysical and electrochemical behavior of the ferrocenyl-substituted benzothiadiazoles show strong donor–acceptor interaction. The increase in the number of acceptor benzothiadiazole unit, results in the lowering of the energy gap, which leads to the bathochromic shift of the absorption spectrum. The single crystal X-ray structures of **3a**, **5a**, and **5g** were obtained which show interesting supramolecular interactions.

INTRODUCTION

There has been a considerable interest in the design, and synthesis of molecular system with enhanced π-electron delocalization for photonic, and electronic applications.[1,2] The linkage of the donor (D) and the acceptor (A) units on the conjugated species results in a D–π–A kind of molecular system.[3] The photonic properties of the D–π–A molecular system can be tuned by either: (a) varying the strength of the donor, or the acceptor group or (b) by changing the π-linker between the donor and the acceptor units.[4,5] A variety of acceptors have been exploited for the design, and synthesis of D–π–A molecular materials.[6] The benzothiadiazole (BTD) with a five-membered heterocyclic ring (C═N–S–N═C) is a strong acceptor, due to its high electron affinity.[7,8] Our group has explored ferrocenyl moiety as a strong electron donor, for variety of photonic applications.[9,10] Recently, we have synthesized symmetrically substituted ferrocenyl BTDs.[11] Our group is interested in modulating the π-bridges between the donor, and the acceptor units, and varying the number of acceptor, in order to explore its photonic, and electronic properties. In this paper, we report the synthesis of the unsymmetrical D–π_1–A–π_2–D and the symmetrical D–π_1–A–π_2–A–π_1–D type of BTD systems. A set of new bromo-BTDs were designed and synthesized, which serve as the precursors for the synthesis of the ferrocenyl-substituted BTDs. The structural, photophysical, and electrochemical properties of these BTD systems were explored.

RESULT AND DISCUSSION

The ferrocenyl substituted BTDs **5a**–**5h** were synthesized by the Pd-catalyzed Sonogashira, and Stille coupling reactions. The dibromo-BTD **2** was synthesized by the bromination reaction of the BTD **1**.[12] The precursors **3a**–**3c** were synthesized by the Pd-catalyzed Sonogashira coupling reactions of the dibromo-BTD **2**, with the corresponding ferrocenyl acetylenes (Scheme 1). The reaction of the 1 equivalent of dibromo-BTD **2**, with 1.1 equivalents of ethynyl-ferrocene (**a**), 4- ferrocenylphenylacetylene (**b**), and 3-ferrocenylphenylacetylene (**c**) under the Sonogashira coupling conditions resulted **3a**, **3b**, and **3c** in 60%, 50%, and 55% yield respectively.[13] The use of more than 1.1 equivalents of the ferrocenyl acetylenes resulted in the formation of the disubstituted BTDs **4a**–**4c** in major quantity (≥40%), whereas the use of less than 1.1 equivalents of alkynyl-ferrocene left unreacted dibromo-BTD **2**.

The Sonogashira coupling reaction of the ferrocenyl-substituted bromo-BTDs **3a**–**c** and the ferrocenyl acetylenes resulted in BTDs **5a**–**f** in 60–70% yield (Schemes 2 and 3). The Stille coupling reaction of the precursor **3a** with bis-(tributylstannyl)acetylene and 2,5-bis(tributylstannyl)thiophene resulted in **5g** and **5h** in 30% and 25% yield, respectively (Scheme 2).[14] All the compounds were well characterized by ^{1}H and ^{13}C NMR and HRMS techniques. The ^{1}H NMR spectra of the

Received: March 19, 2013
Published: April 30, 2013

dx.doi.org/10.1021/jo4005734 | J. Org. Chem. 2013, 78, 4940–4948

Scheme 1. Synthetic Route for BTD Precursors 3a−c

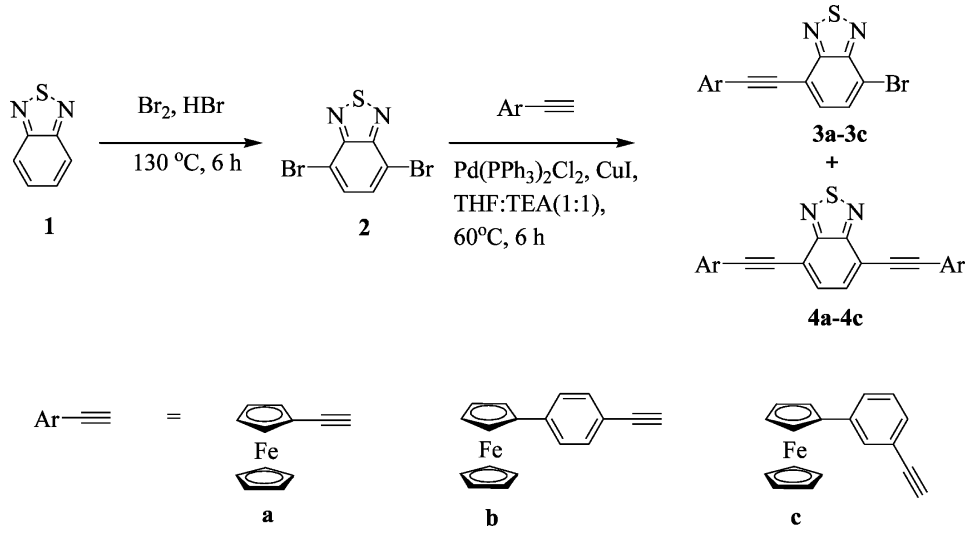

precursors **3a−c** show two characteristic doublets between 7.86 and 7.19 ppm corresponding to the two protons of the BTD. The BTDs **5a−d,g,h** show the characteristic doublet for the BTD protons in the region 7.80−7.50 ppm. The BTD **5e** exhibits a multiplet for the two protons between 7.84 and 7.80 ppm, whereas the BTD **5f** shows a singlet at 7.79 ppm for the BTD protons. The BTD **3a**, **5a**, and **5g** were also characterized by single-crystal X-ray diffraction.

Thermogravimetric Analysis. The thermal properties of the BTDs **5a−h** were investigated by the thermogravimetric analysis (TGA) at a heating rate of 10 °C min^{-1} under nitrogen atmosphere (Figure S3, Supporting Information). The decomposition temperatures for 10% weight loss in the BTDs **5a**, **5c**, and **5f** was above 400 °C. The BTDs **5b**, **5d**, and **5e** show the decomposition temperature above 200 °C, whereas the BTDs **5g** and **5h** with two acceptor units show the decomposition temperature above 230 °C. The thermal stability trend reveals that the ferrocenyl substituted BTDs with two acceptor BTD units have lower thermal stability.

X-ray Analysis. The single crystal of the ferrocenyl BTDs **3a**, **5a**, and **5g** were obtained via slow diffusion of ethanol into the dichloromethane solution at room temperature. The BTDs **3a** and **5a** crystallizes in the triclinic space group $P\bar{1}$, whereas the BTD **5g** with two acceptor unit crystallizes in the monoclinic space group $P2_1/c$. Figure 1 shows the single-crystal X-ray structure of **3a**, **5a**, and **5g**.

The BTD core shows planar structure in **3a**, **5a**, and **5g**. The two acceptor units in BTD **5g** are oriented anti to each other. The cyclopentadienyl rings of the ferrocenyl moiety shows eclipsed conformation in BTDs **3a** and **5a** and eclipsed skew conformation in BTD **5g**. The crystal structure of **3a** consists of two molecules in an asymmetric unit where the Br atom is labeled as Br1 and Br2. The dihedral angle between the planes containing the BTD core, and the cyclopentadienyl ring of ferrocene units was found to be 60.06° (for Br1), and 58.41° (for Br2) in **3a**, 12.90° (for Fe1), and 87.68° (for Fe2) in **5a**, and 56.66° (Fe1) in **5g**. The important bond lengths, and bond angles are listed in the Table S2a−c (see the Supporting Information for details).

The packing diagram of **3a** exhibits short S1···N2 (3.131 Å), S2···N4 (3.154 Å), and N4···N4 (3.080 Å) interhetroatom contacts between the BTD rings, which leads to the formation of dimer in head-to-head fashion.[15] These dimers are interconnected through hydrogen bonding between N1···H10 (2.640 Å), Br1···H18 (2.934 Å), and Br2···H33 (2.954 Å) to form stacked structures. These stacks are interlinked through CH···π interaction C16H16···C27−C31 (3.056 Å) to form a 2D zigzag chain (Figure 2 and Figure 2a, Supporting Information).

The packing diagram of **5a** shows intermolecular C−H···N interaction C33−H33···N2 (2.665 Å), which leads to the formation of a hydrogen bonded dimers in head-to-head fashion. These dimers are interlinked through C−H···π interaction of C4H4···C17−C21 (3.046 Å) to form a 1D polymeric chain. The C−H···π interaction C31H31··· C22−C26 (2.803) leads to the cross-linking of the chains and formation of a 2D sheetlike structure (Figure 3).

The packing diagram of BTD **5g** shows intermolecular C−H···N interaction between the H14 of one BTD molecule and the N1 of the neighboring BTD molecule at a distance of 2.672 Å (Figure 4), which leads to the formation of 1D polymeric chain.

Photophysical Properties. The UV−vis absorption spectra of the BTDs **5a−h** were recorded in dichloromethane at room temperature (Figure 5), and the data are listed in Table 1. The BTDs **5a−h** show strong absorption band between 409 and 489 nm, corresponding to the $\pi\rightarrow\pi^*$ transition.[11] The $\pi\rightarrow\pi^*$ transition exhibits red shift in the absorption maxima with the enhancement of the conjugation length. The ferrocenyl BTDs with two acceptor units show substantial bathochromic shift, and higher molar extinction coefficient (ε) as compared to the BTDs with one acceptor unit. The red shift in the absorption maxima follows the order **5h** > **5g** > **5f** > **5e** > **5d** > **5c** > **5a** > **5b**. The linkage of the donor ferrocene at the *meta*-position of the π-spacer in compound **5b**, and **5e** disrupts the extended π-conjugation, and thus results in blue shift in the absorption maxima compared to their isomers **5a**, and **5f**, respectively.[16] The absorption spectra of BTDs **5a**, **5b**, **5c**, **5g**, and **5h** exhibits band at 507 nm, 504 nm, 515 nm (shoulder), 540 nm, and 542 nm (shoulder), respectively due to the charge transfer from ferrocene to the BTD unit. The BTDs **5d−f** do not show distinct CT band, which may be due to the overlap of the charge-transfer absorption with the $\pi\rightarrow\pi^*$ absorption.[11,17] The interpretation of the absorption spectra reveals that the charge transfer is more pronounced, when the donor ferrocene unit is attached to BTD unit by acetylenic linkage. This is also reflected

dx.doi.org/10.1021/jo4005734 | J. Org. Chem. 2013, 78, 4940−4948

Scheme 2. Synthetic Route for Ferrocenyl BTDs 5a−c,g,h[a]

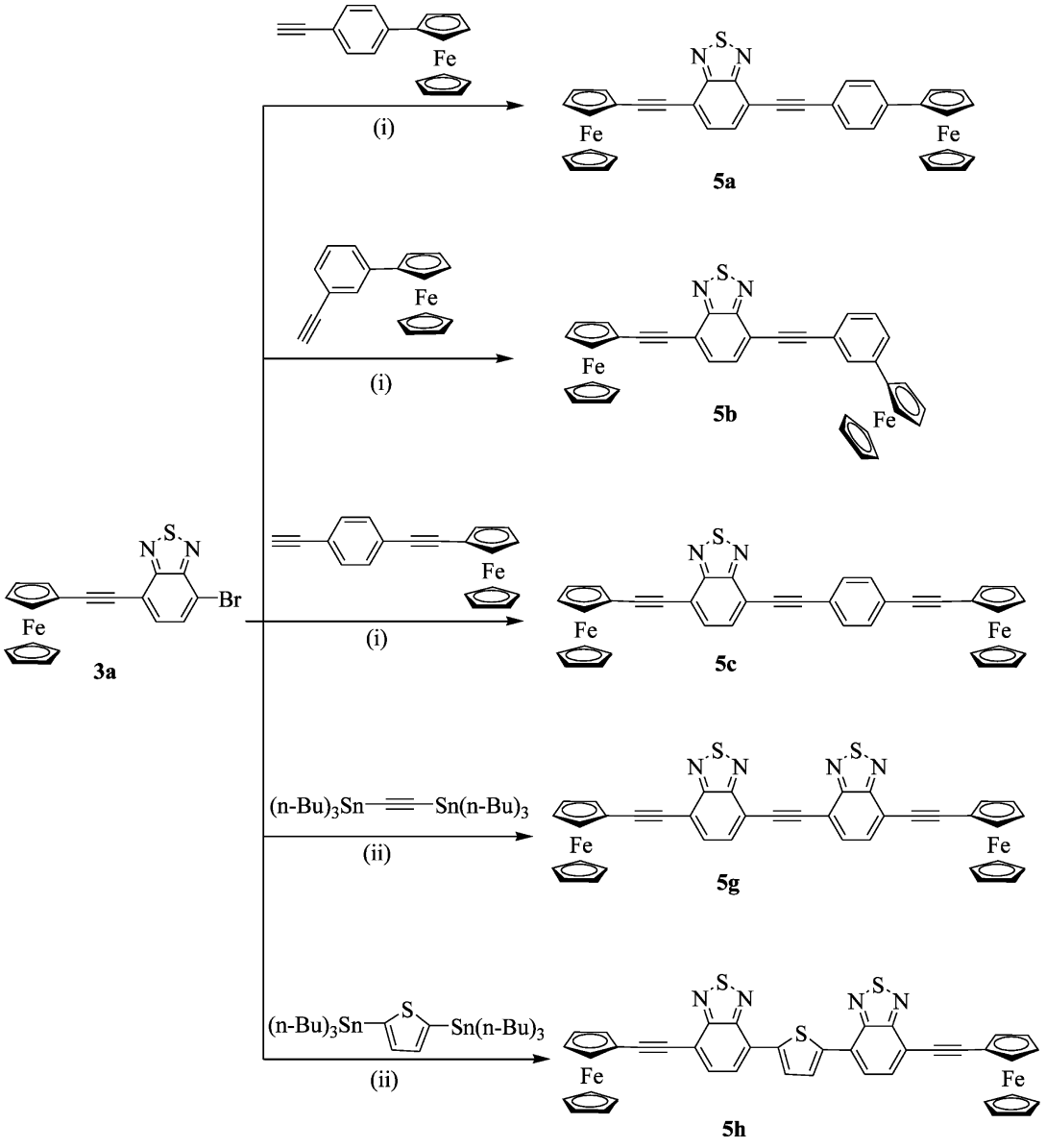

[a]Reaction conditions: (i) $Pd(PPh_3)_2Cl_2$, CuI, THF/TEA (1:1), 60 °C, 6 h; (ii) $Pd(PPh_3)_4$, toluene, 100 °C, 15 h.

from the intense red colored dichloromethane solution of BTDs **5a−h** (Figure 6).[18] The emission studies of BTDs **5a−h** shows complete quenching of the fluorescence.[19] This further confirms the strong donor−acceptor interaction in these BTD systems.[20]

Electrochemical Properties. The electrochemical behavior of the BTDs **5a−5h** were explored by the cyclic voltammetric (CV), and differential pulse voltammetric analysis in dry dichloromethane (DCM) solution at room temperature using tetrabutylammoniumhexafluorophosphate ($TBAPF_6$) as a supporting electrolyte. The electrochemical data of the BTDs **5a−h** are listed in Table 1, and the representative cyclic voltammograms are shown in Figure 7. The BTDs **5a** and **5b** exhibit two reversible oxidation waves in the region 0.02−0.12 V, whereas the BTDs **5c−h** exhibit one reversible oxidation wave in the region 0.07 to 0.16 V, corresponding to the oxidation of ferrocene to ferrocenium ion. The ferrocenyl moiety in the BTDs **5a−h** exhibit harder oxidation potential compared to free ferrocene, confirming the strong electronic communication between the ferrocene unit, and the BTD core.[21] The trend in the oxidation potential of the ferrocenyl moiety in the BTDs **5a−5h** follows the order **5g** > **5h**> **5c** > **5a** > **5f** > **5b** > **5e** > **5d**, which reveals that the increase in the number of acceptor unit improves the donor−acceptor interaction.

The BTDs **5a−f** exhibit one-electron reversible reduction wave in the region −1.59 to −1.67 V corresponding to the BTD acceptor moiety, whereas the BTDs **5g−h** exhibit two distinct waves in the region −1.55 to −1.77 V due to the presence of two acceptor units. This indicates strong intramolecular electronic interaction between the two BTD units in BTDs **5g** and **5h**, which leads to a decrease of the first reduction potential.[22,23] In general, the reduction potential for the BTDs **5a−h** shows lower values compared to unsubstituted BTD **1** (−1.98 V vs Fc/Fc^+ in DCM) indicating that the BTD ring in ferrocenyl-substituted BTDs is easy to reduce compared to unsubstituted BTD.[11,24] The reversibility was observed with peak current ratios close to 1 for all processes, and the deviation from 1 is the result of baseline

dx.doi.org/10.1021/jo4005734 | J. Org. Chem. 2013, 78, 4940−4948

Scheme 3. Synthetic Route for Ferrocenyl BTDs 5d–f[a]

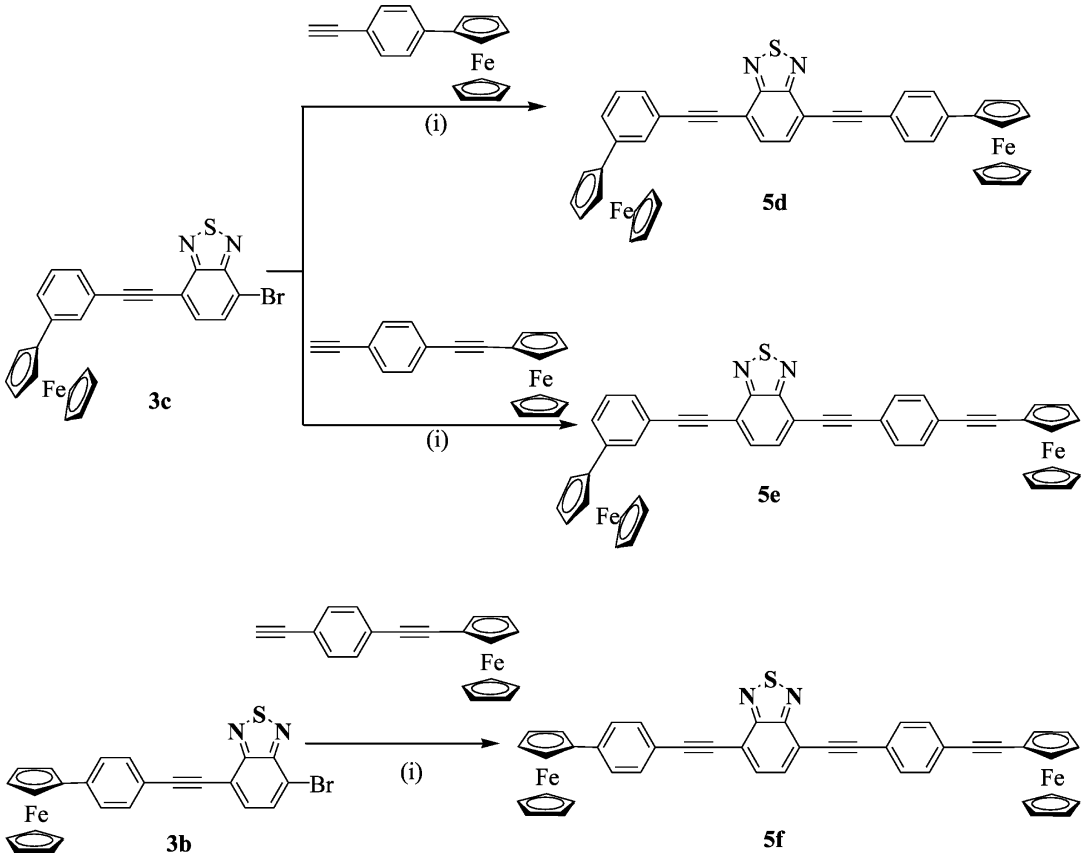

[a]Reaction condition: (i) $Pd(PPh_3)_2Cl_2$, CuI, THF/TEA (1:1), 60 °C, 6 h.

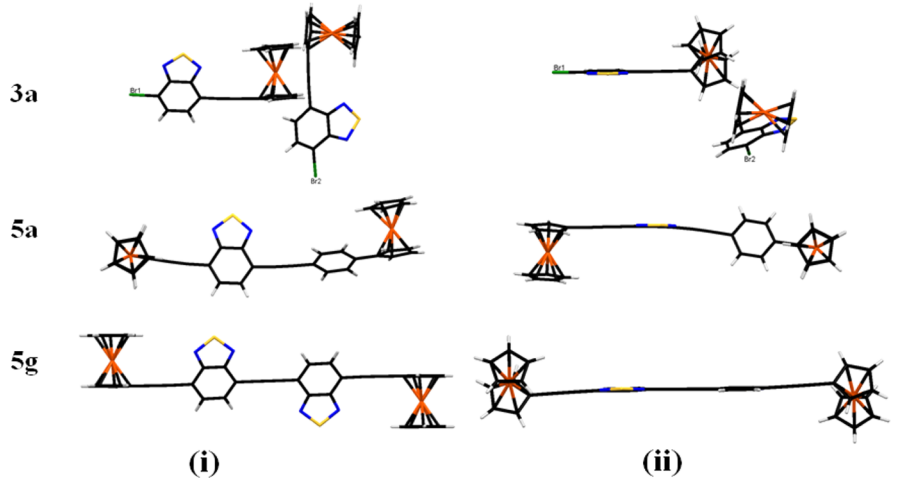

Figure 1. Single-crystal X-ray structure of ferrocenyl BTDs **3a**, **5a**, and **5g**: (i) top view and (ii) side view.

uncertainty due to the onset of solvent decomposition at these low potentials.[25]

Theoretical Calculations. In order to explore the electronic structure of the unsymmetrical and symmetrical BTDs, DFT calculations was performed on the BTDs **5a** and **5g**. The contours of the HOMO and LUMO of BTDs **5a** and **5g** are shown in Figure 8, which reveals that the HOMO orbitals are localized over ferrocene, benzene, and benzo of the BTD unit. The HOMOs of BTD **5a** and **5g** was found to be at almost same energy level. The LUMOs orbitals of BTD **5a** and **5g** are mainly concentrated on the BTD unit.[22] The lowering of the LUMO energy level for BTD **5g** in comparison to BTD **5a** can be attributed to the presence of two acceptor units.[26] The lower energy gap in the BTD **5g** as compared to BTD **5a** results in the bathochromic shift in the electronic absorption.

■ CONCLUSION

In summary, a donor–acceptor system was designed, where donor is ferrocene and acceptor is benzothiadiazole, and synthesized by the Pd-catalyzed Sonogashira and Stille coupling reaction. The modulation of the π-spacer group between the

dx.doi.org/10.1021/jo4005734 | J. Org. Chem. 2013, 78, 4940–4948

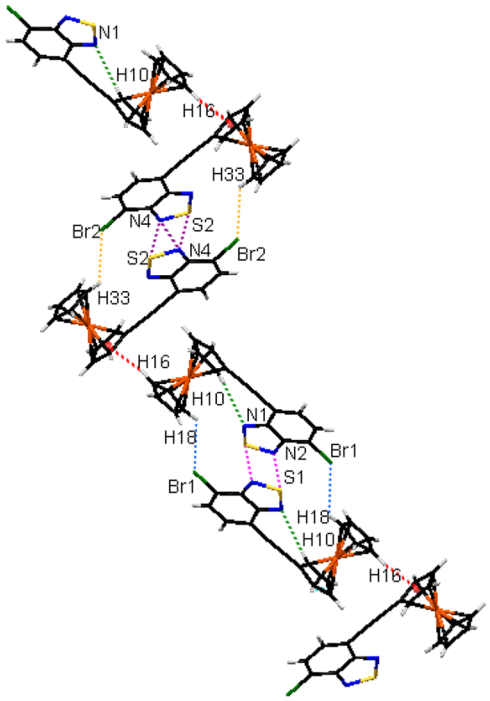

Figure 2. Packing diagram of ferrocenyl BTD **3a** forming 2D-network along the *a*-axis.

donor and the acceptor units and increasing the number of acceptor units results in significant perturbation in the photonic properties. The photophysical and electrochemical properties of the BTDs exhibit strong donor−acceptor interaction. The detailed nonlinear optical characterization of these ferrocenyl-substituted BTDs is currently ongoing in our laboratory.

EXPERIMENTAL SECTION

Chemicals were used as received unless otherwise indicated. All oxygen- or moisture-sensitive reactions were performed under nitrogen/argon atmosphere using standard Schlenk method. Triethylamine (TEA) was received from commercial source and distilled on KOH prior to use. ^{1}H NMR (400 MHz), and ^{13}C NMR (100 MHz) spectra were recorded on 400 MHz, using $CDCl_3$ as solvent. Tetramethylsilane (TMS) was used as reference for recording ^{1}H (of residual proton; δ = 7.26 ppm) and ^{13}C (δ = 77.0 ppm) spectra in $CDCl_3$. The ^{1}H NMR splitting patterns have been described as "s, singlet; bs, broad singlet; d, doublet; t, triplet; and m, multiplet". UV−vis absorption spectra of all compounds were recorded in DCM. Cyclic voltamograms (CVs) and differential pulse voltamograms (DPVs) were recorded on an electrochemical analyzer using a glassy carbon as working electrode, Pt wire as the counter electrode, and saturated calomel electrode (SCE) as the reference electrode. The scan rate was 100 mVs^{-1} for CV and 50 mVs^{-1} for DPV. A solution of tetrabutylammonium hexafluorophosphate ($TBAPF_6$) in CH_2Cl_2 (0.1 M) was employed as the supporting electrolyte. DCM was freshly distilled from CaH_2 prior to use. All potentials were experimentally referenced against the saturated calomel electrode couple but were then manipulated to be referenced against Fc/Fc+ as recommended by IUPAC.[27] Under our conditions, the Fc/Fc+ couple exhibited i_{pc}/i_{pa} = 0.94, E° = 0.38 V versus SCE. HRMS was recorded on a TOF-Q mass spectrometer.

General Procedure for the Preparation of Ferrocenyl Bromo-BTDs 3a−c by Sonogashira Coupling Reaction. To a stirred solution of the respective alkynylferrocene (0.37 mmol) and 4,7-dibromo-BTD (0.34 mmol) in THF and TEA (1:1, v/v) were added $PdCl_2(PPh_3)_2$ (10 mg, 0.014 mmol) and CuI (2 mg, 0.01 mmol) under an argon flow at room temperature. The reaction mixture was stirred for 6 h at 60 °C and then cooled to room temperature. The solvent was evaporated under reduced pressure, and the mixture was purified by SiO_2 chromatography with DCM/hexane (1:3, v/v) followed by recrystallization in DCM/methanol (1:1) to obtain a colored solid.

*4-Bromo-7-ferrocenylethynylbenzo[1,2,5]thiadiazole (**3a**):* red solid (86.4 mg, yield 60%); mp 170.5−171.2 °C; ^{1}H NMR (400 MHz, $CDCl_3$, δ in ppm) 7.65 (d, 1H, J = 8.3 Hz), 7.20 (d, 1H, J = 8.0 Hz), 4.49 (s, 2H), 4.24 (bs, 7H); ^{13}C NMR (100 MHz, $CDCl_3$, δ in ppm) 154.2, 153.1, 132.1, 132.0, 117.4, 113.5, 97.0, 81.1, 71.9, 70.2, 69.4, 63.9; HRMS (ESI) m/z calcd for $C_{18}H_{11}BrFeN_2S$ 421.9172 [M^+], found 421.9168 [M^+].

*4-Bromo-7-(4-ferrocenylphenylethynyl)benzo[1,2,5]thiadiazole (**3b**):* red solid (85 mg, yield 50%); mp 182.2−183.4 °C; ^{1}H NMR (400 MHz, $CDCl_3$, δ in ppm) 7.83 (d, 1H, J = 7.5 Hz), 7.66 (d, 1H, J = 7.5 Hz), 7.56 (d, 2H, J = 8.5 Hz), 7.48 (d, 2H, J = 8.5 Hz), 4.68 (t, 2H, J = 1.8 Hz), 4.37 (t, 2H, J = 1.8 Hz), 4.04(s, 5H); ^{13}C NMR (100 MHz, $CDCl_3$, δ in ppm) 154.2, 153.1, 141.1, 132.5, 132.0, 125.8, 119.4, 117.0, 114.3,

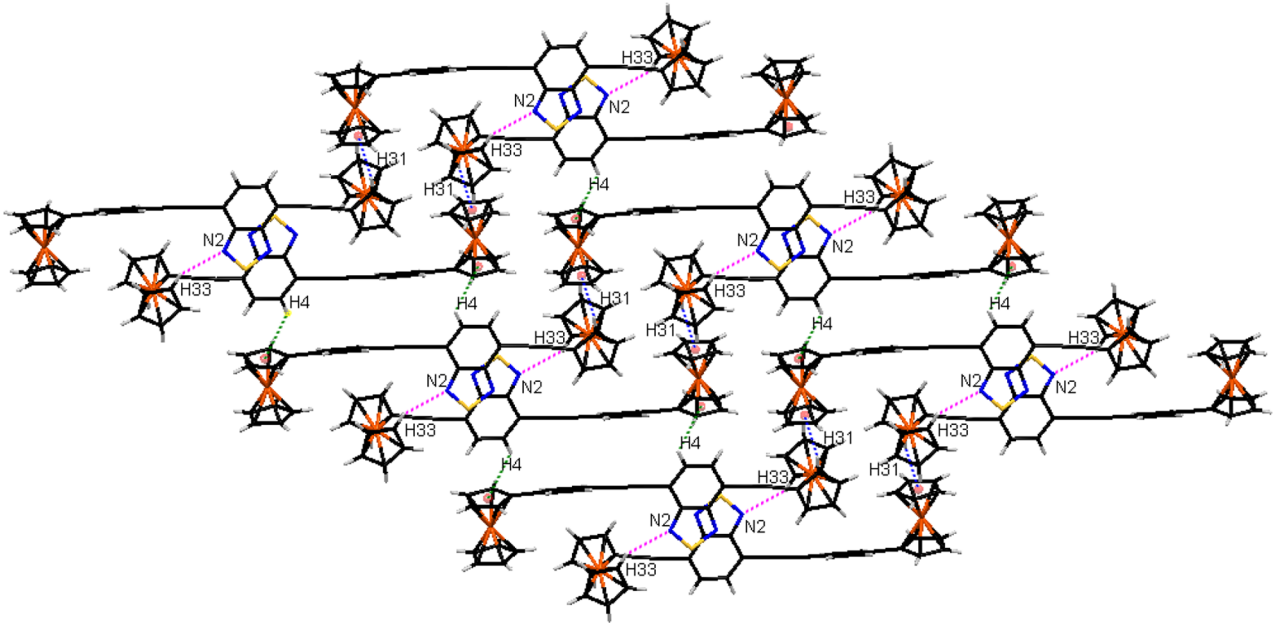

Figure 3. Packing diagram of ferrocenyl BTD **5a** along the *b*-axis.

dx.doi.org/10.1021/jo4005734 | J. Org. Chem. 2013, 78, 4940−4948

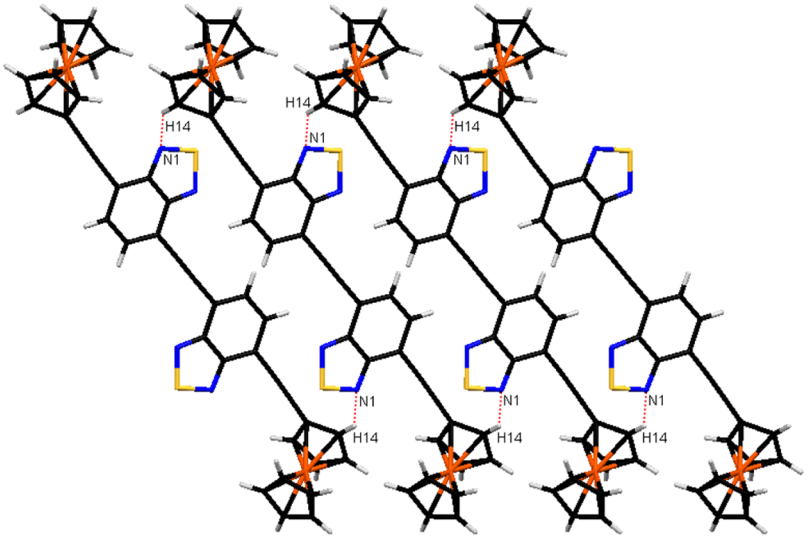

Figure 4. Packing diagram of ferrocenyl BTD **5g** along the *c*-axis.

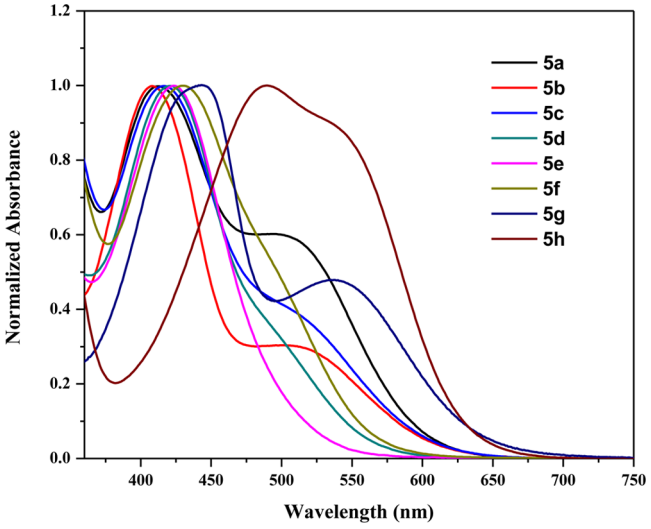

Figure 5. Normalized electronic absorption spectra of ferrocenyl BTD **5a–h** in dichloromethane at 1.0×10^{-6} M concentration.

97.5, 84.7, 83.9, 69.76, 69.75, 69.5, 66.6; HRMS (ESI) *m*/*z* calcd for $C_{24}H_{15}BrFeN_2S$ 499.9467 [M^+], found 499.9464 [M^+].

*4-Bromo-7-(3-ferrocenylphenylethynyl)benzo[1,2,5]thiadiazole (**3c**):* orange solid (93.5 mg, yield 55%); mp 148.2–148.8 °C; ^{1}H NMR (400 MHz, $CDCl_3$, δ in ppm) 7.85 (d, 1H, J = 7.5 Hz), 7.73 (t, 1H, J = 1.3 Hz), 7.70 (d, 1H, J = 7.8 Hz), 7.51–7.47 (m, 2H), 7.31 (t, 1H, J = 1.3 Hz), 4.68 (t, 2H, J = 1.8 Hz), 4.34 (t, 2H, J = 1.8 Hz), 4.06 (s, 5H); ^{13}C NMR (100 MHz, $CDCl_3$, δ in ppm) 154.2, 153.1, 139.9, 132.9, 132.0, 129.4, 129.0, 128.5, 126.9, 122.3, 116.7, 114.6, 97.1, 84.3, 84.0, 69.7, 69.2, 66.5; HRMS (ESI) *m*/*z* calcd for $C_{24}H_{15}BrFeN_2S$ 497.9485 [M^+], found 497.9515 [M^+].

General Procedure for the Preparation of Ferrocenyl BTDs 5a–f by Sonogashira Coupling Reaction. To a stirred solution of respective alkynylferrocene (0.37 mmol) and ferrocenyl bromo-BTDs **3a**/**3b**/**3c** (0.34 mmol) in THF and TEA (1:1, v/v) were added $PdCl_2(PPh_3)_2$ (10 mg, 0.014 mmol), and CuI (2 mg, 0.01 mmol) under an argon flow at room temperature. The reaction mixture was stirred for 6 h at 60 °C and then cooled to room temperature. The solvent was then evaporated under reduced pressure, and the mixture was purified by SiO_2 chromatography with DCM/hexane (2:3, v/v) followed by recrystallization in DCM/methanol (1:1) to obtain a colored solid.

*4-Ferrocenylethynyl-7-(4-ferrocenylphenylethynyl)benzo[1,2,5]-thiadiazole (**5a**):* red solid (149 mg, yield 70%); mp >300.0 °C; ^{1}H NMR (400 MHz, $CDCl_3$, δ in ppm) 7.76 (d, 1H, J = 7.5 Hz), 7.73 (d, 1H, J = 7.3 Hz), 7.58 (d, 2H, J = 8.5 Hz), 7.48 (d, 2H, J = 8.8 Hz), 4.69 (t, 2H, J = 2 Hz), 4.64 (t, 2H, J = 1.8 Hz), 4.37 (t, 2H, J = 2 Hz), 4.32–4.30 (m, 7H), 4.04 (s, 5H); ^{13}C NMR (100 MHz, $CDCl_3$, δ in ppm) 154.5, 154.4, 140.9, 132.3, 132.0, 131.8, 125.8, 119.6, 117.8, 116.6, 97.72, 97.68, 84.0, 82.0, 71.9, 70.2, 69.8, 69.51, 69.45, 66.6, 64.2; HRMS (ESI) *m*/*z* calcd for $C_{36}H_{24}Fe_2N_2S$ 628.0355 [M^+], found 628.0387 [M^+]; UV/vis (DCM) λ_{max} (ε [M^{-1} cm^{-1}]) 413 (38250), 507 (22677).

*4-Ferrocenylethynyl-7-(3-ferrocenylphenylethynyl)benzo[1,2,5]-thiadiazole (**5b**):* orange-red solid (138 mg, yield 65%); mp 208.5–

Table 1. Photophysical and Electrochemical Data of the Ferrocenyl BTDs 5a–h

	photophysical data[a]		electrochemical data[b]		
compd	λ_{abs} (nm)	ε (M^{-1} cm^{-1})	wave	$E°$ (V)	i_{pc}/i_{pa}
Ferrocene			1	0.00	0.94
5a	413	38250	1[d]	0.12	
	507	22677	2[d]	0.02	
			3	−1.66	0.97
5b	409	39850	1[d]	0.11	
	504	12870	2[d]	0.02	
			3	−1.67	0.91
5c	417	52950	1	0.14	0.97[c]
	515	sh	2	−1.64	0.98[c]
5d	421	46400	1	0.07	0.99
			2	−1.62	0.98[c]
5e	423	54630	1	0.09	0.96
			2	−1.60	0.95
5f	429	52500	1	0.11	0.98
			2	−1.59	0.95[c]
5g	443	69000	1	0.16	0.98
	540	33023	2	−1.55	0.91
			3	−1.72	0.89[c]
5h	489	70900	1	0.15	0.94[c]
	542	sh	2	−1.62	0.93[c]
			3	−1.77	0.84[c]

[a]Absorbance measured in dichloromethane at 4×10^{-6} M concentration; sh = shoulder; λ_{abs}: absorption wavelength; ε: extinction coefficient. [b]Recorded by cyclic voltammetry, in 0.1 M solution of $TBAPF_6$ in DCM at 100 mVs^{-1} scan rate, vs Fc/Fc^+ at 25 °C; i_{pc}/i_{pa} = peak current ratio. [c]i_{pa}/i_{pc}; [d]Recorded by differential pulse voltammetry.

dx.doi.org/10.1021/jo4005734 | J. Org. Chem. 2013, 78, 4940–4948

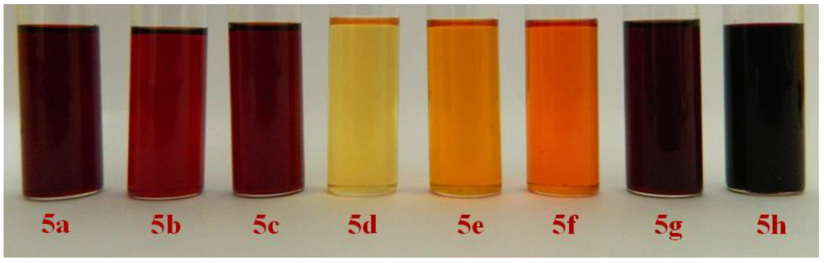

Figure 6. Ferrocenyl BTDs **5a–h** at 10^{-4} M concentration in DCM.

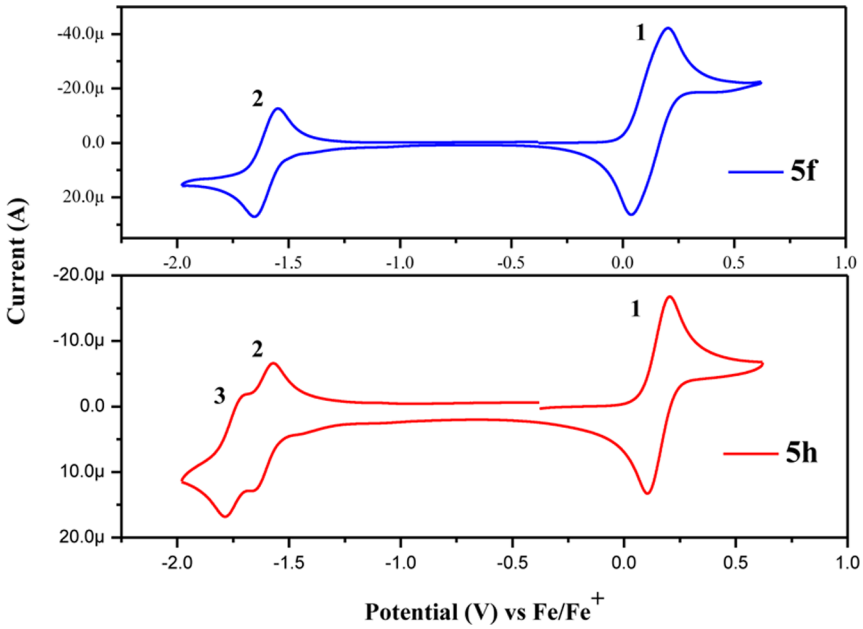

Figure 7. Cyclic voltammogram of ferrocenyl BTDs **5f** and **5h** at 0.01 M concentration in 0.1 M $TBAPF_6$ in dichloromethane recorded at a scan rate of 100 mV s^{-1}.

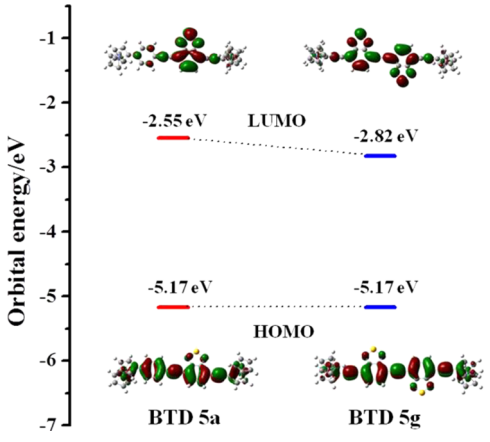

Figure 8. Correlation diagram showing the HOMO, and LUMO wave functions and energies of the BTDs **5a** (left) and **5g** (right), as determined at the B3LYP/6-31G** level (isovalue = 0.02).

209.6 °C; ^{1}H NMR (400 MHz, $CDCl_3$, δ in ppm) 7.80 (d, 1H, J = 7.5 Hz), 7.75–7.74 (m, 2H), 7.51–7.48 (m, 2H), 7.31 (t, 1H, J = 7.8 Hz), 4.69 (t, 2H, J = 1.8 Hz), 4.65 (t, 2H, J = 2 Hz), 4.34–4.31 (m, 9H), 4.06 (s, 5H); ^{13}C NMR (100 MHz, $CDCl_3$, δ in ppm) 154.5, 154.4, 139.9, 132.7, 131.8, 129.5, 129.1, 128.5, 126.8, 122.6, 118.0, 116.3, 97.8, 97.3, 85.2, 84.1, 81.9, 72.0, 70.2, 69.7, 69.5, 69.2, 66.5, 64.1; HRMS (ESI) m/z calcd for $C_{36}H_{24}Fe_2N_2S$ 628.0355 [M^+], found 628.0370 [M^+]; UV/vis (DCM) λ_{max} (ε [M^{-1} cm^{-1}]) 409 (39850), 504 (12870).

*4-Ferrocenylethynyl-7-(4-ferrocenylethynylphenylethynyl)benzo-[1,2,5]thiadiazole (**5c**):* red solid (137 mg, yield 62%); mp >300.0 °C; ^{1}H NMR (400 MHz, $CDCl_3$, δ in ppm) 7.76 (d, 1H, J = 7.3 Hz), 7.73 (d, 1H, J = 7.3 Hz), 7.61 (d, 2H, J = 8 Hz), 7.49 (d, 2H, J = 8 Hz), 4.64 (t, 2H, J = 2 Hz), 4.51 (t, 2H, J = 1.8 Hz), 4.33–4.30 (m, 7H), 4.26–4.25 (m, 7H); ^{13}C NMR (100 MHz, $CDCl_3$, δ in ppm) 154.38, 154.37, 132.6, 131.8, 131.7, 131.3, 124.6, 121.6, 118.1, 116.1, 98.0, 97.0, 91.2, 87.1, 85.5, 81.9, 72.0, 71.5, 70.2, 70.0, 69.5, 69.0, 64.8, 64.1; HRMS (ESI) m/z calcd for $C_{38}H_{24}Fe_2N_2S$ 652.0355 [M^+], found 652.0364 [M^+]; UV/vis (DCM) λ_{max} (ε [M^{-1} cm^{-1}]) 417(52950), 515 (sh).

*4-(3-Ferrocenylphenylethynyl)-7-(4-ferrocenylphenylethynyl)-benzo[1,2,5]thiadiazole (**5d**):* orange solid (143 mg, yield 60%); mp 210.5–211.4 °C; ^{1}H NMR (400 MHz, $CDCl_3$, δ in ppm) 7.83 (d, 1H, J = 7.5 Hz), 7.80 (d, 1H, J = 7.5 Hz), 7.75 (t, 1H, J = 1.8 Hz), 7.59 (d, 2H, J = 8.5 Hz), 7.52–7.48 (m, 4H), 7.32 (t, 1H, J = 7.8 Hz), 4.69 (t, 4H, J = 2 Hz), 4.37 (t, 2H, J = 2 Hz), 4.35 (t, 2H, J = 2 Hz), 4.05–4.06 (m, 10H); ^{13}C NMR (100 MHz, $CDCl_3$, δ in ppm) 154.44, 154.41, 141.0, 139.9, 132.6, 132.2, 132.1, 129.5, 129.1, 128.5, 126.8, 125.8, 122.5, 119.5, 117.5, 116.9, 114.1, 98.2, 97.6, 85.5, 85.1, 84.1, 83.9, 69.8, 69.7, 69.5, 69.2, 66.6, 66.5; HRMS (ESI) m/z calcd for $C_{42}H_{28}Fe_2N_2S$ 704.0688 [M^+], found 704.0704 [M^+]; UV/vis (DCM): λ_{max} (ε [M^{-1} cm^{-1}]) 421(46,400).

*4-(4-Ferrocenylethynylphenylethynyl)-7-(3-ferrocenyl-phenylethynyl)benzo[1,2,5]thiadiazole (**5e**):* orange solid (148 mg, yield 60%); mp 219.5–220.6 °C; ^{1}H NMR (400 MHz, $CDCl_3$, δ in ppm) 7.84–7.80 (m, 2H), 7.75 (s, 1H), 7.62 (d, 2H, J = 7.8 Hz), 7.51–7.49 (m, 4H), 7.32 (t, 1H, J = 7.8 Hz), 4.69 (s, 2H), 4.52 (s, 2H), 4.35–4.20 (m, 9H), 4.06 (s, 5H); ^{13}C NMR (100 MHz, $CDCl_3$, δ in ppm) 154.3, 144.8, 139.9, 132.52, 132.45, 131.9, 131.3, 129.5, 129.1, 128.5, 126.9, 124.8, 122.5, 121.5, 117.3, 117.1, 97.9, 97.4, 91.3, 86.9, 85.5, 84.1, 71.5, 70.0, 69.7, 69.2, 69.1, 66.5, 64.8, 60.6; HRMS (ESI) m/z calcd for

dx.doi.org/10.1021/jo4005734 | J. Org. Chem. 2013, 78, 4940–4948

$C_{44}H_{28}Fe_2N_2S$ 728.0668 [M^+], found 728.0665 [M^+]; UV/vis (DCM) λ_{max} (ε [M^{-1} cm^{-1}]) 423(54,630).

*4-(4-Ferrocenylethynylphenylethynyl)-7-(4-ferrocenylphenylethynyl)benzo[1,2,5]thiadiazole (**5f**):* orange solid (151 mg, yield 61%); mp >300.0 °C; ^{1}H NMR (400 MHz, $CDCl_3$, δ in ppm) 7.79 (s, 2H), 7.62 (d, 2H, J = 8.5 Hz), 7.58 (d, 2H, J = 8.5 Hz), 7.51−7.47 (m, 4H), 4.69 (t, 2H, J = 1.8 Hz), 4.51 (t, 2H, J = 1.8 Hz), 4.37 (t, 2H, J = 2 Hz), 4.26−4.25 (m, 7H), 4.04 (s, 5H); ^{13}C NMR (100 MHz, $CDCl_3$, δ in ppm) 154.4, 148.4, 132.5, 132.2, 132.1, 131.9, 131.4, 128.0, 125.9, 124.8, 123.7, 122.3, 121.5, 119.5, 116.8, 91.2, 85.5, 83.9, 81.5, 71.5, 70.0, 69.8, 69.6, 69.1, 66.6, 64.8; HRMS (ESI) m/z calcd for $C_{44}H_{28}Fe_2N_2S$ 728.0668 [M^+], found 728.0664 [M^+]; UV/vis (DCM) λ_{max} (ε [M^{-1} cm^{-1}]) 429 (52500).

General Procedure for the Preparation of Ferrocenyl BTDs 5g and 5h by Stille Coupling Reaction. To a stirred solution of BTD **3a** (0.5 mmol) in toluene (20 mL) were added $Pd(PPh_3)_4$ (0.05 mmol) and the respective stannyl derivative (0.25 mmol) under an argon flow at room temperature. The mixture was stirred for 15 h at 100 °C and then allowed to cool to room temperature. The solvent was evaporated under reduced pressure, and the black residue was dissolved in dichloromethane (20 mL). This was washed with brine solution (2 × 20 mL). The aqueous layer was washed with more dichloromethane (20 mL), the combined organic layers were dried with Na_2SO_4 and filtered, and the dichloromethane was allowed to evaporate. The resulting residual solid was purified by column chromatography through silica gel (100−200 mesh) with DCM as the eluent. The desired compound eluted in DCM. The solvent was evaporated, and the solid was recrystallized from DCM/methanol (1:1) to give a colored solid.

*1,2-Bis(7-ferrocenylethynylbenzothidiazole-4-yl)ethyne (**5g**).* reddish-brown solid (106 mg, yield 30%); mp >300.0 °C; ^{1}H NMR (400 MHz, $CDCl_3$, δ in ppm) 7.92 (d, 2H, J = 7.3 Hz), 7.77 (d, 2H, J = 7.3 Hz), 4.65 (t, 4H, J = 1.8 Hz), 4.34−4.31 (m, 14); ^{13}C NMR (100 MHz, $CDCl_3$, δ in ppm) 154.38, 154.36, 133.2, 131.7, 118.8, 115.5, 92.8, 82.0, 72.0, 70.3, 69.6, 68.0, 64.0; HRMS (ESI) m/z calcd for $C_{38}H_{22}Fe_2N_4S_2$ 709.9981 [M^+], found 710.0035 [M^+]; UV/vis (DCM): λ_{max} (ε [M^{-1} cm^{-1}]) 443 (69000), 540 (33023).

*1,2-Bis(7-ferrocenylethynylbenzothidiazole-4-yl)thiophene (**5h**):* purple solid (96 mg, yield 25%); mp >300.0 °C;^{1}H NMR (400 MHz, $CDCl_3$, δ in ppm) 8.25 (s, 2H), 7.94 (d, 2H, J = 7.5 Hz), 7.79 (d, 2H, J = 7.5 Hz), 4.66 (t, 4H, J = 1.5), 4.33−4.32 (m, 14H); ^{13}C NMR (100 MHz, $CDCl_3$, δ in ppm) 155.2, 151.9, 140.8, 132.2, 128.9, 126.52, 125.3, 116.5, 96.8, 82.2, 72.0, 70.4, 69.5, 65.8, 60.4; HRMS (ESI) m/z calcd for $C_{40}H_{24}Fe_2N_4S_3$ calcd 767.9858 [M^+], found 767.9832 [M^+]; UV/vis (DCM) λ_{max} (ε [M^{-1} cm^{-1}]) 489 (70900), 542 (sh).

■ ASSOCIATED CONTENT

Supporting Information

Characterization data for all the new compounds. Copies of ^{1}H, ^{13}C NMR, and HRMS spectra of new compounds, crystallographic information files (CIFs) for compounds **3a**, **5a**, and **5g**. This material is available free of charge via the Internet at http://pubs.acs.org.

■ AUTHOR INFORMATION

Corresponding Author

*E-mail: rajneeshmisra@iiti.ac.in.

Notes

The authors declare no competing financial interest.

■ ACKNOWLEDGMENTS

R.M. thanks CSIR and DST, New Delhi, for financial support. We are grateful to Sophisticated Instrumentation Centre (SIC) Single Crystal X-ray diffraction Facility, IIT Indore.

■ REFERENCES

(1) (a) Kato, S.; Furuya, T.; Kobayashi, A.; Nitani, M.; Ie, Y.; Aso, Y.; Yoshihara, T.; Tobita, S.; Nakamura, Y. *J. Org. Chem.* **2012**, *77*, 7595−7606. (b) Omer, K. M.; Ku, S. Y.; Wong, K. T.; Bard, A. J. *J. Am. Chem. Soc.* **2009**, *131*, 10733−10741. (c) Sonar, P.; Singh, S. P.; Li, Y.; Soh, M. S.; Dodabalapur, A. *Adv. Mater.* **2010**, *22*, 5409−5413. (d) Li, Y.; Li, A.-Y.; Li, B.-X.; Huang, J.; Zhao, L.; Wang, B.-Z.; Li, J.-W.; Zhu, X.-H.; Peng, J.; Cao, Y.; Ma, D.-G.; Roncali, J. *Org. Lett.* **2009**, *11*, 5318−5321. (e) Kobayashi, N.; Inagaki, S.; Nemykin, V. N.; Nonomura, T. *Angew. Chem., Int. Ed.* **2001**, *40*, 2710−2712.

(2) (a) Kato, S.; Matsumoto, T.; Ishi-i, T.; Thiemann, T.; Shigeiwa, M.; Gorohmaru, H.; Maeda, S.; Yamashitad, Y.; Mataka, S. *Chem. Commun.* **2004**, 2342−2343. (b) Neto, B. A. D.; Lapis, A. A. M.; Júnior, E. N.; da, S.; Dupont, J. *Eur. J. Org. Chem.* **2013**, 228−255. (c) Kato, S.; Matsumoto, T.; Shigeiwa, M.; Gorohmaru, H.; Maeda, S.; Ishi-i, T.; Mataka, S. *Chem.—Eur. J.* **2006**, *12*, 2303−2317. (d) Wang, J.-L.; Tang, Z.-M.; Xiao, Q.; Ma, Y.; Pei, J. *Org. Lett.* **2009**, *11*, 863−866. (e) Lindner, B. D.; Engelhart, J. U.; Märken, M.; Tverskoy, O.; Appleton, A. L.; Rominger, F.; Hardcastle, K. I.; Enders, M.; Bunz, U. H. F. *Chem.—Eur. J.* **2012**, *18*, 4627−4633. (f) Aviram, A.; Ratner, M. A. *Chem. Phys. Lett.* **1974**, *29*, 277−283.

(3) (a) Tang, Z. M.; Lei, T.; Jiang, K. J.; Song, Y. L.; Pei, J. *Chem. Asian J.* **2010**, *5*, 1911−1917. (b) Wu, Y.; Zhu, W. *Chem. Soc. Rev.* **2013**, *42*, 2039−2058.

(4) Wang, J.-L.; Xiao, Q.; Pei, J. *Org. Lett.* **2010**, *12*, 4164−4167.

(5) (a) Zhang, H.; Wan, X.; Xue, X.; Li, Y.; Yu, A.; Chen, Y. *Eur. J. Org. Chem.* **2010**, 1681−1687. (b) Bures, F.; Schweizer, W. B.; May, J. C.; Boudon, C.; Gisselbrecht, J.-P.; Gross, M.; Biaggio, I.; Diederich, F. *Chem.—Eur. J.* **2007**, *13*, 5378−5387.

(6) (a) Zhou, E.; Yamakawa, S.; Tajima, K.; Yang, C.; Hashimoto, K. *Chem. Mater.* **2009**, *21*, 4055−4061. (b) Hrobárik, P.; Hrobáriková, V.; Sigmundová, I.; Zahradník, P.; Fakis, M.; Polyzos, I.; Persephonis, P. *J. Org. Chem.* **2011**, *76*, 8726−8736. (c) Janowska, I.; Miomandre, F.; Clavier, G.; Audebert, P.; Zakrzewski, J.; Thi, K. H.; Ledoux-Rak, I. *J. Phys. Chem. A* **2006**, *110*, 12971−12975. (d) Lembo, A.; Tagliatesta, P. *J. Phys. Chem. A* **2006**, *110*, 11424−11433. (e) Zhu, W.; Wu, G. S. *J. Phys. Chem. A* **2001**, *105*, 9568−9574. (f) Zhu, Y.; Wolf, M. O. *J. Am. Chem. Soc.* **2000**, *122*, 10121−10125.

(7) (a) Sakurai, H.; Ritonga, M. T. S.; Shibatani, H.; Hirao, T. *J. Org. Chem.* **2005**, *70*, 2754−2762. (b) Dhanabalan, A.; van Duren, J. K. J.; van Hal, P. A.; van Dongen, J. L. J.; Janssen, R. A. J. *Adv. Funct. Mater.* **2001**, *11*, 255−262. (c) Zhang, M.; Tsao, H. N.; Pisula, W.; Yang, C.; Mishra, A. K.; Müllen, K. *J. Am. Chem. Soc.* **2007**, *129*, 3472−3473.

(8) (a) Shi, C. J.; Yao, Y.; Yang, Y.; Pei, Q. B. *J. Am. Chem. Soc.* **2006**, *128*, 8980−8986. (b) Hou, Q.; Zhou, Q. M.; Zhang, Y.; Yang, W.; Yang, R. Q.; Cao, Y. *Macromolecules* **2004**, *37*, 6299−6305. (c) Zhu, Z.; Waller, D.; Gaudiana, R.; Morana, M.; Muhlbacher, D.; Scharber, M.; Brabec, C. *Macromolecules* **2007**, *40*, 1981−1986. (d) Thomas, K. R. J.; Lin, J. T.; Velusamy, M.; Tao, Y. T.; Chuen, C. H. *Adv. Funct. Mater.* **2004**, *14*, 83−90.

(9) (a) Gautam, P.; Dhokale, B.; Shukla, V.; Singh, C. P.; Bindra, K. S.; Misra, R. *J. Photochem. Photobiol., A Chem.* **2012**, *239*, 24−27. (b) Jadhav, T.; Maragani, R.; Misra, R.; Sreeramulu, V.; Rao, D. N.; Mobin, S. M. *Dalton Trans.* **2013**, *42*, 4340−4342. (c) Maragani, R.; Thaksen, J.; Mobin, S. M.; Misra, R. *RSC Adv.* **2013**, *3*, 2889−2892.

(10) (a) Gautam, P.; Dhokale, B.; Mobin, S. M.; Misra, R. *RSC Adv.* **2012**, *2*, 12105−12107. (b) Dhokale, B.; Gautam, P.; Mobin, S. M.; Misra, R. *Dalton Trans.* **2013**, *42*, 1512−1518. (c) Sharma, R.; Maragani, R.; Mobin, S. M.; Misra, R. *RSC Adv.* **2013**, *3*, 5785−5788.

(11) Misra, R.; Gautam, P.; Sharma, R.; Mobin, S. M. *Tetrahedron Lett.* **2013**, *54*, 381−383.

(12) Wang, B.; Tsang, S.; Zhang, W.; Tao, Y.; Wong, M. S. *Chem. Commun.* **2011**, *47*, 9471−9473.

(13) Ma, X.; Hua, J.; Wu, W.; Jin, Y.; Meng, F.; Zhan, W.; Tian, H. *Tetrahedron* **2008**, *64*, 345−350.

(14) Wang, X.; Sun, Y.; Chen, S.; Guo, X.; Zhang, M.; Li, X.; Li, Y.; Wang, H. *Macromolecules* **2012**, *45*, 1208−1216.

(15) (a) Chen, S.; Li, Y.; Yang, W.; Chen, N.; Liu, H.; Li, Y. *J. Phys. Chem. C* **2010**, *114*, 15109−15115. (b) Anant, P.; Lucas, N. T.; Jacob, J. *Org. Lett.* **2008**, *10*, 5533−5536. (c) Pop, F.; Amacher, A.; Avarvari, N.; Ding, J.; Daku, L. M. L.; Hauser, A.; Koch, M.; Hauser, J.; Liu, S.; Decurtins, S. *Chem.—Eur. J.* **2013**, *19*, 2504−2514.

(16) (a) Melinger, J. S.; Pan, Y.; Kleiman, V. D.; Peng, Z.; Davis, B. L.; McMorrow, D.; Lu, M. *J. Am. Chem. Soc.* **2002**, *124*, 12002−12012. (b) Misra, R.; Kumar, R.; Chandrashekar, T. K.; Suresh, C. H.; Nag, A.; Goswami, D. *J. Am. Chem. Soc.* **2006**, *128*, 16083−16091.
(17) Ziessel, R.; Retailleau, P.; Elliott, K. J.; Harriman, A. *Chem.—Eur. J.* **2009**, *15*, 10369−10374.
(18) Rao, M. R.; Kumar, K. V. P.; Ravikanth, M. *J. Organomet. Chem.* **2010**, *695*, 863−869.
(19) (a) Fery-Forgues, S.; Delavaux-Nicot, B. *J. Photochem. Photobiol., A* **2000**, *132*, 137−159. (b) Dhokale, B.; Gautam, P.; Misra, R. *Tetrahedron Lett.* **2012**, *53*, 2352−2354. (c) Nadtochenko, V. A.; Denisov, N. N.; Gak, V. Y.; Abramova, N. V.; Loim, N. M. *Russ. Chem. Bull.* **1999**, *148*, 1900−1903. (d) Barlow, S.; Marder, S. R. *Chem. Commun.* **2000**, 1555−1562.
(20) Sharma, R.; Gautam, P.; Mobin, S. M.; Misra, R. *Dalton Trans.* **2013**, *42*, 5539−5545.
(21) Maragani, R.; Jadhav, T.; Mobin, S. M.; Misra, R. *Tetrahedron* **2012**, *68*, 7302−7308.
(22) (a) Xu, E.; Zhong, H.; Lai, H.; Zeng, D.; Zhang, J.; Zhu, W.; Fang, Q. *Macromol. Chem. Phys.* **2010**, *211*, 651−656. (b) Watanabe, M.; Goto, K.; Fujitsuka, M.; Tojo, S.; Majima, T.; Shinmyozu, T. *Bull. Chem. Soc. Jpn.* **2010**, *83*, 1155−1161.
(23) Poander, L. E.; Pandey, L.; Barlow, S.; Tiwari, P.; Risko, C.; Kippelen, B.; Bredas, J. L.; Marder, S. R. *J. Phys. Chem. C* **2011**, *115*, 23149−23163.
(24) Watanabe, M.; Goto, K.; Shibahara, M.; Shinmyozu, T. *J. Org. Chem.* **2010**, *75*, 6104−6114.
(25) Auger, A.; Muller, A. J.; Swarts, J. C. *Dalton Trans.* **2007**, 3623−3633.
(26) Patel, D. G. D.; Feng, F.; Ohnishi, Y.-y.; Abboud, K. A.; Hirata, S.; Schanze, K. S.; Reynolds, J. R. *J. Am. Chem. Soc.* **2012**, *134*, 2599−2612.
(27) Gritzner, G.; Kuta, G. *J. Pure Appl. Chem.* **1984**, *56*, 461−466.